69th International Astronautical Congress, Bremen, Germany. Copyright © 2018 by the authors. All rights reserved.

IAC–18–C1.9.11x44026

Tour Design Techniques for the Europa Clipper Mission

Stefano Campagnola
Jet Propulsion Laboratory, California Institute of Technology, stefano.campagnola@jpl.nasa.gov

Brent B. Buffington, Try Lam, Anastassios E. Petropoulos, Etienne Pellegrini
Jet Propulsion Laboratory, California Institute of Technology

Europa is one of the most scientifically interesting targets of the solar system, as it may possess the three necessary ingredients for life: an extensive ocean of liquid water, an energy source from tidal heating, and a suite of biogenic elements. To explore the habitability of Europa, NASA is developing the Europa Clipper mission, currently scheduled to be launched in 2022. Europa resides deep inside the gravity well of Jupiter, in a region of the magnetosphere with many trapped ionized particles that get accelerated to near relativistic speeds; a Europa orbiter mission would require a large amount of ΔV for an orbit insertion maneuver, and would only return limited science data before being critically exposed to radiation. To mitigate these issues, Europa Clipper instead only utilizes Europa flybys, connected by Europa-resonant and non-resonant orbits. Science data is collected during high-radiation passes, and returned to Earth during the rest of the Jovian orbits, at a much lower radiation dose exposure. This paper will present several tour tools techniques developed for the design of the Europa Clipper flyby trajectory. In particular, the paper will describe different ways to perform fast line-of-apsides rotations; a new approach to improve the coverage of Europa's trailing and leading edges, with the lighting conditions considerations; parametric studies of the expected radiation dose and time-of-flight as function of the Europa resonance; and a quick way to estimate the radiation dose for Jovian tours. Other techniques, that were already presented in previous papers, will be reviewed for completeness. We then implement some of the new approaches in the 18F17 tour.

I. Introduction

Planetary satellites are some of the most intriguing targets for planetary science, as they hold the keys to understand the origin of the solar system and often possess the potential ingredients for life.[1] Satellite exploration missions are enabled by complex, winding trajectories, called satellite or moon tours, that can last years but have characteristic time scales of days (the orbit periods of the satellites). Tours use tens of flybys to attain both close-up science observations and to change the spacecraft orbit around the planet. Their design is challenging because of the large number of flybys (which increases the dimension of the design space while imposing tight encounter constraints) and because of the many operational and environmental requirements. In addition, the spacecraft motion is perturbed by the non-spherical gravity harmonics of the planet, by the gravitational pull of multiple satellites acting at the same time, and for large orbits, by the Sun gravity. The optimization of even a single end-to-end moon tour in a high-fidelity model is a difficult, time-consuming task, and completely exploring such a chaotic, high-dimensional solution space is impractical. Instead, mission analysts have developed advanced techniques in simplified models to search for high quality tour options with high science return and adhere to ground system and flight system requirements while mitigating mission risks prior to ultimately converging in a high-fidelity flight software. These techniques helped mission analyst to design tours for Galileo, Europa Clipper, Cassini, JUICE, and for several proposed missions to Neptune, Uranus, among others. Yet more advanced tour design techniques are needed, as space missions becomes more complex, building on the success of Galileo and Cassini. For example, in preparation to the Critical Design Review (CDR) in 2019, the Europa Clipper project is designing new tours with more science return, enhanced robustness, but subject to the same requirements levied on the mission design from the ground system (i.e., operational cadence types of requirements) and flight system, compared to the Preliminary Design Review (PDR) baseline tour 17F12.[2]

This will paper present new techniques that enable the design of higher quality tours, specifically, including: a quick way to estimate the radiation dose for Jovian tours; parametric studies of the expected radiation dose and time-of-flight as function of the

Europa resonance; different ways to perform fast line-of-apsides rotations; and a new approach to improve the coverage of Europa's trailing and leading edges, with lighting conditions considerations. An example tour, 18F17-beta, is discussed to exhibit the results of utilizing these techniques in order to attain the desired tour enhancements.

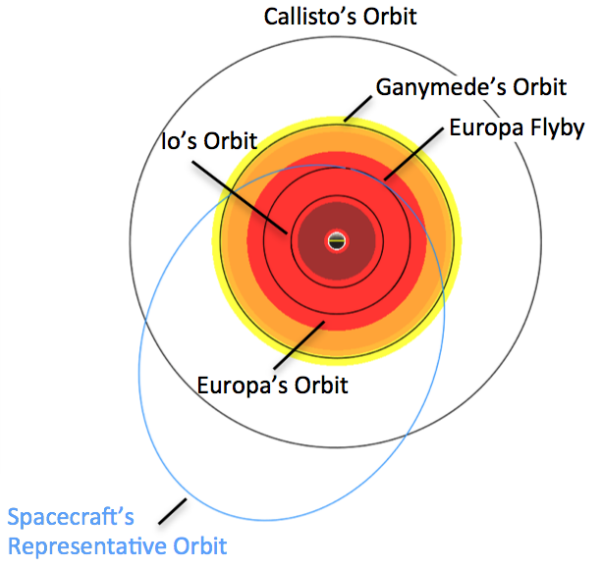

Fig. 1: Radiation Environment and Overall Mission Design Strategy. Representative orbit with a 14.2-day period. Approximately 70% of the orbit is spent outside the harsh radiation environment (˜10 days).[3]

II. Background

II.i Europa Clipper mission and typical tours

Europa resides deep within Jupiter's gravity well, in a region of the magnetosphere with many trapped ionized particles that get accelerated to near relativistic speeds, creating a radiation environment that is detrimental to unprotected spacecraft electronics; as such, a Europa orbiter mission would only return limited science data before being critically exposed to radiation and would also require a large amount of propellant to insert into orbit around Europa. To mitigate these issues, Europa Clipper Mission will instead execute a high number of Europa flybys in a highly eccentric orbit around Jupiter. The flight system will collect a large volume of science data at each Europa flyby (where the radiation will be the strongest), and then quickly escape the intense radiation environment near Europa to downlink the Europa science data to Earth over the remainder of Jovian orbit, when the radiation levels are very low (Fig. 1).

The Europa Clipper architecture is thus enabled by a tour with more than 40 Europa flybys designed to attain global-regional coverage under specific solar illumination conditions, relative velocity, and range, which vary depending on the instrument performing the measurements. After a 300-km Ganymede flyby and a large Jupiter insertion maneuver (JOI), all Europa Clipper tour designs start with a ˜200-day capture orbit followed by 5 phases:[2,4,5]

1. The Pump-Down Phase, where Ganymede flybys reduce the orbit period and inclination, and target the first Europa flyby with the right geometry and illumination conditions;[6]

2. The Europa Campaign 1 (EC-1) Phase, where Europa flybys mostly at 2-week cadence provide observations over the lit, anti-Jovian hemisphere. The location of EC-1 flybys range from $L_{Eu} \approx -15^o$ to $L_{Eu} \approx 60^o$, where L_{Eu} is the projection of the Sun-Jupiter-Europa angle on Europa's orbit*;

3. The Transition to Europa Campaign 2 Phase, where the Europa Clipper orbits and the location of the Europa flybys are rotated of 180^o;

4. The Europa Campaign 2 (EC-2) Phase, where Europa flybys provide observation over the lit sub-Jovian hemisphere, and over the night-side anti-Jovian hemisphere;

5. The Disposal Phase, where the spacecraft is designed to impact Jupiter.

The current baseline tour, 17F12, was the first tour adopted by the Project that was designed to meet (most of) the 300+ constraints levied on trajectory design by the NASA-selected payload and by the flight system. For CDR the Mission Design Team is designing new tours, that would maintain the current quality of 17F12 in terms of science return and mission costs and risks, but could also include with the following enhancements:

Enhancement 1: $\geq$ 1 pass over Europa's leading point region (within 15^o from 0^o lat, 270^o E Long), at $<$ 2000 km altitude, and with local solar time (LST) between 9^h and 15^h.

*More precisely, $L_{(ga)}$ is argument of latitude of the gravity assist moon, measured from the projection of the Jupiter-Sun direction on the moon's orbital plane.

Enhancement 2: increase the time-of-flight between between the first and second Europa flyby to ≥ 2 months, for instrument calibration and to test the flight system in the Europa environment; also include some robustness to missed flyby observations.

Enhancement 3: a lower flyby cadence to reduce the operational complexities, if possible.

The remainder of this section describes some of the previously developed tour techniques. The subsequent sections of this paper present a candidate tour that meets these three goals (at varying levels), and the specific techniques developed for its design.

II.ii Standard tour design techniques

Tour design techniques are developed in low-fidelity models to allow broad searches of solutions in lower-dimensional spaces. The techniques are used to design portions of the tour that serve as an initial guess for high-fidelity trajectory optimization software. The model used in this paper is patched conics, where the trajectory is split in conic orbits, patched by instantaneous ΔV's, to simulate each satellite flyby. In addition, the moon orbits are assumed to be circular and coplanar, although an extension of the techniques to moon ephemerides is sometimes possible.

Pump and crank angles

In patched conics, a flyby rotates the spacecraft velocity relative to the moon ($\mathbf{v}_\infty$) following well-know hyperbolic orbit formulas $\mathrm{v}_\infty^+ = f(\mathrm{v}_\infty^-, \mathbf{p})$, where $\mathbf{p}$ are two flyby parameters such as altitude and B-plane angle. Note that by conservation of Keplerian energy of the flyby hyperbola, $v_\infty \triangleq \|\mathbf{v}_\infty^+\| = \|\mathbf{v}_\infty^-\|$. v_∞ coordinates are conveniently referred to a rotating frame, where the x-axis is from the moon to the planet, and the y-axis is opposite to the moon velocity $\mathbf{v}_{ga}$. For moons in near-circular orbits that are also tidally locked, as is the case for Europa (and the majority of the moons in our solar system), this reference frame is almost aligned with the moon body-fixed frame (with the x-axis towards the prime meridian and the z-axis towards the north pole). The spherical coordinates of v_∞ are its magnitude v_∞, the pump angle α (angle between $\mathbf{v}_\infty$ and $\mathbf{v}_{ga}$), and the crank angle κ , as shown in Fig. 2.

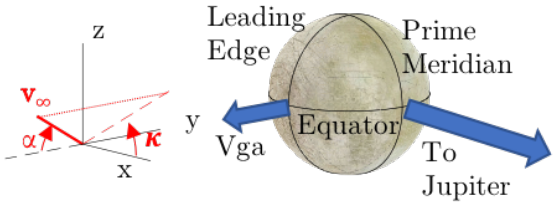

Fig. 2: $\mathbf{v}_\infty$ vector in with the pump α and crank κ angles, and the body-fixed reference frame of tidally-locked moon on circular orbits.

Resonant and non-resonant transfers

Each conic transfer in the tour is determined by the epoch t and the v_∞ of the flyby at the beginning of the leg (departure) or at the end of the leg (arrival). When the departure and arrival moons are the same, then the corresponding v_∞'s are also the same (this can be shown by simple symmetry, but it's also a consequence of the conservation of energy in the moon-planet-spacecraft CR3BP[7]), and the transfer is either resonant, non-resonant, or $n\pi$-transfer.[8]

In a resonant transfer, the departure and arrival flybys occur at the same moon orbit location, and the period of the spacecraft is commensurable to the period of the moon. Resonant transfers are denoted by the resonant ratio $\rho = n : m$, where n is the number of moon revolutions and m is the number of spacecraft revolutions (in some literature, the resonant ratio is defined as $m : n$). It is easy to show that for a given v_∞, the resonant ratio only depends on the pump angle ($\rho \longleftrightarrow \alpha$). Also it can be shown, that resonant transfers only exist for $v_\infty \geq v_{\infty,min}(\rho)$.

In a non-resonant transfer, the departure and arrival flybys do not occur at the same moon orbit locations, and as such, require the transfer to be co-planar with the moon's orbit. Non-resonant transfers are denoted as $n : m^+$ (long) or $n : m^-$(short), depending if the transfers is longer or shorter than $2m\pi$.

Finally in π-transfers the departure and arrival flybys are 180^o apart. π-transfers are typically inclined.

The v_∞ sphere

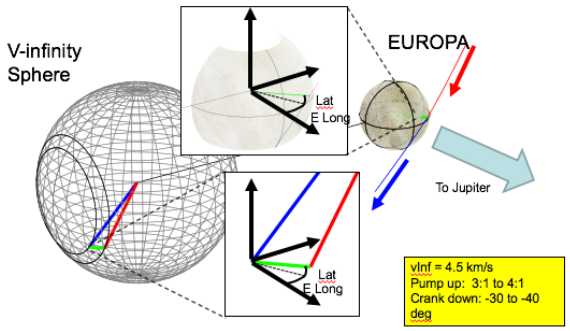

Fig. 3: Example of flyby on the v_∞ sphere and in position space

The $\mathbf{v}_\infty$ sphere is the locus of all possible instances of the $\mathbf{v}_\infty$ vector during a sequence of flybys at the same moon. A particular sequence is represented by a two-dimensional discrete dynamical system in (α, κ). For example, flybys are mapping $(\alpha^+, \kappa^+)^{(i)} = \tilde{f}(\alpha^-, \kappa^-, \mathbf{p})^{(i)}$, resonant transfers are mappings $(\alpha^-, \kappa^-)^{(i+1)} = (\alpha^+, \kappa^+)^{(i)}$, and non-resonant transfers are mapping $(\alpha^-, \kappa^-)^{(i+1)} = (\alpha^+, \pi - \kappa^+)^{(i)}$.

Figure 3 shows an example of "pump-up/crank-down" flyby, that is, a flyby that increases the period by *reducing* the pump angle, and also reduces the crank angle. The figure shows the corresponding flyby in position space; the closest approach longitude and latitude can be determined directly from the pump and crank angles with simple formulas.[9] The flyby $\Delta\mathbf{v} = \mathbf{v}_\infty^+ - \mathbf{v}_\infty^-$ is opposite to the radius vector at closest approach. Finally the figure also shows the locus of resonant transfers, which is a circle on the sphere (level sets of α), in a plane perpendicular to the satellite velocity. A crank-only flyby would then be represented with a Δv connecting two points on the same resonant circle; the Δv and the closest approach vector would be perpendicular to the satellite velocity, so the closest approach would be along the prime or 180^o meridian[†].

Sequence of flybys: Resonant Hopping, Petal Rotations, Crank-over-the-top Sequences, and Switch-Flip

Resonant hopping is a technique that utilizes one or more resonant transfers to increase (pump up) or decrease (pump down) the resonant ratio beyond the level attainable with a single, minimum-altitude flyby.

Petal rotation is a tour design technique that utilizes a series of non-resonant transfers that alternate between pumping up and pumping down to rotate the spacecraft orbit.[10] They are grouped in families, each identified by a pair of non-resonant transfers $n_1 : m_1^+ / n_2 : m_2^-$, and are parametrized by v_∞. The rotations are clockwise if $\rho_1 > \rho_2$, and anti-clockwise if $\rho_1 < \rho_2$.

Crank-over-the-top sequences (COTs) are a series resonant transfers that begin and end with equatorial flybys ($\kappa = 0^o$ or $\kappa = 180^o$), and traverse a full 180^o in crank angle, typically, but not always, using a fixed α. If the COT starts at $\kappa = 0^o$, it covers the sub-planet hemisphere of the moon with retrograde flybys centered at 0^o E long, from north to south if $\Delta\kappa < 0$ and from south to north if $\Delta\kappa > 0$. If the COT sequence starts at $\kappa = 180^o$, it covers the anti-planet hemisphere of the moon with direct flybys centered at 180^o E long, from north to south if $\Delta\kappa > 0$ and from south to north if $\Delta\kappa < 0$. For more details see.[4]

A $\pi-$transfer sequences is a sequence of flybys that move the location of the flyby $\sim 180^o$ along the satellite orbit. The sequence consists of 1) half-COT to crank up the inclination and to to set up a π transfer; 2) the π transfer, where the flyby location is changed by 180^0 on the satellite's orbit; 3) another half-COT to crank-down the inclination. A switch-flip is a technique to attain the same type of rotation, using a $\pi-$transfer at a different moon (for example, the switch-flip of 17F12 consists of a transfer from Europa to Callisto, a Callisto π-transfer sequence, and a transfer from Callisto back to Europa).

III. Tour 18F17-beta

The 18F17-beta tour is a fully integrated trajectory consisting of 45 Europa, 6 Ganymede, and 9 Callisto flybys that would be executed over the course of 4 years (disposal phase excluded, Fig. 4 and Table 1). The tour was first built and optimized in jTOP[11] using a high-fidelity model and then validated in JPL's flight-fidelity software, COSMIC. The different subphases of the tour are:

Pump-Down: Uses Ganymede resonant hopping to pump down the spacecraft orbit to setup a near-equatorial transfer to Europa, with periapsis towards the Jupiter-Sun direction.

COT-1: Uses a 4:1 COT to cover the sunlit anti-Jovian hemisphere of Europa from north to

[†]In a high fidelity model, libration will cause closest approach slightly away from meridians at times

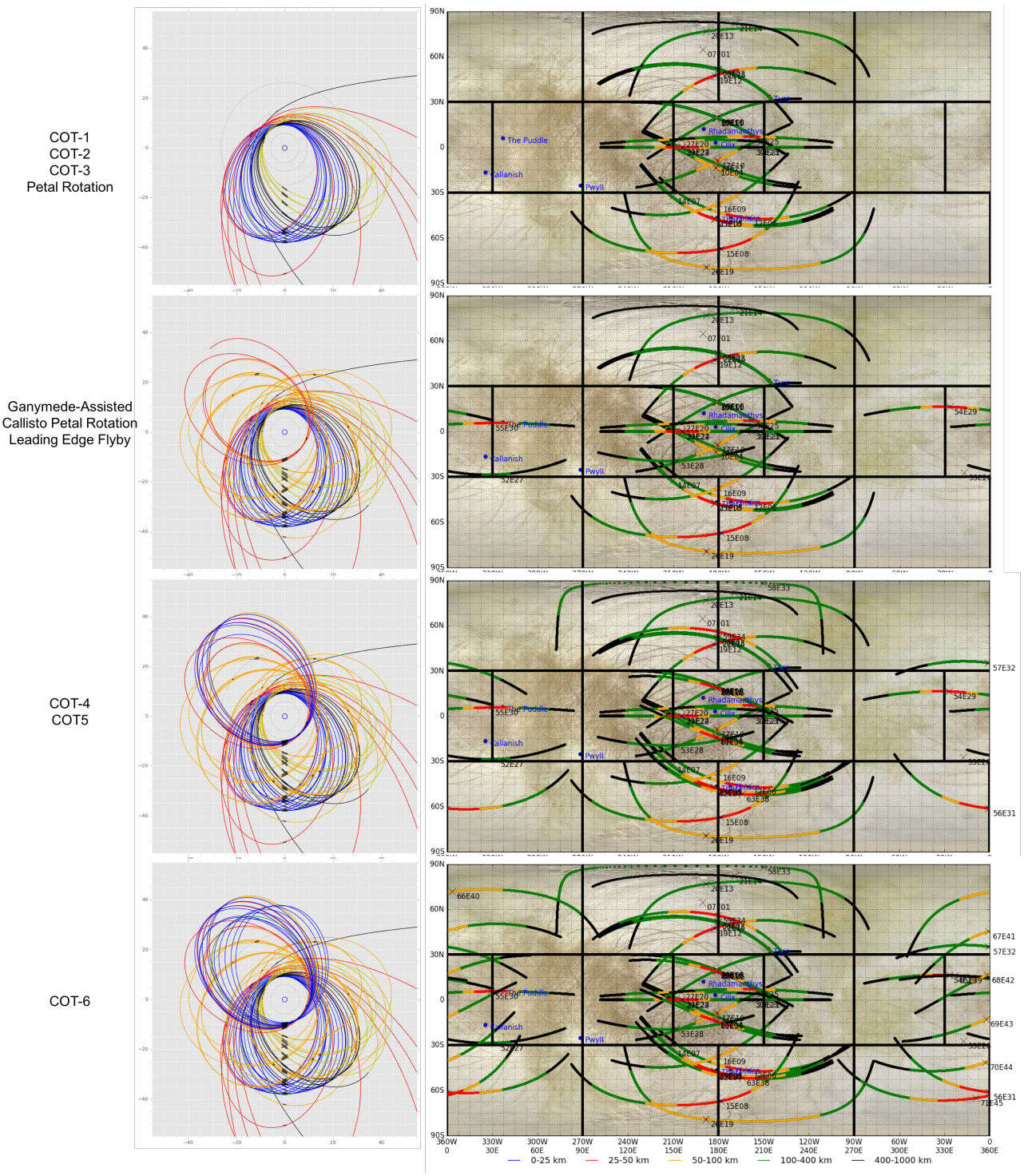

Fig. 4: Trajectory and groundtrack buildup for 18F17-beta. The trajectory is shown from Jupiter's northern hemisphere, centered in Jupiter with the y axis towards the Sun and the z axis toward the normal to the orbit plane. Red: pump-down; blue: COT-1 and COT-2; black: COT-3; yellow: petal rotation; orange: transition, leading edge, and COT-4; blue: COT-5 and COT-6; black: disposal

Mission Phase		Flyby	I/O	Date (ET)	ALT (km)	VINF (km/s)	LST	LAT (deg)	LON (deg)	SEP (deg)	PHS (deg)	TRA (deg)	INC (deg)	PER (days)	BREV nrev	SREV nrev	dTID kRad	TID MRad	dDV m/s	DV m/s	dTOF (days)	TOF (days)	SJB (deg)	κ- deg	κ+ deg	α- deg	α+ deg
Transition to Eu. Campaign 1	Capt.	G00	I	23-Dec-2024 12:46:07	500	7.68	16:46:38	-0	237	162	71.7	-44	4.18	203	28.3	1.25	0.81	0	983.9	0	202	0	11.7	-9.43	-8.84	57.33	63.14
	PumpDown	00G01	O	13-Jul-2025 16:10:20	50	6.27	02:01:50	51	302	14	121	48.3	1.28	76.4	32	3.01	18	0.02	15.08	15.08	229	202.1	85.9	168.3	177.2	60.8	66.5
		01G02	O	27-Feb-2026 16:53:57	871.6	6.56	23:55:37	12	285	126	166	60.3	0.42	35.8	5	1	40.8	0.06	2.77	17.85	35.8	431.2	71	177.8	179.4	69.01	75.9
		04G03	O	04-Apr-2026 11:14:38	919.6	6.54	23:14:49	6.3	279	91	166	70.3	0.03	21.5	3	1	20.3	0.08	0	17.85	21.5	466.9	67.7	179.5	-180	75.55	82.51
		05G04	O	25-Apr-2026 22:19:34	450.7	6.56	22:37:32	7.3	271	72	158	83.2	0.64	13.9	1.81	0.78	30.5	0.11	0	17.85	13	488.4	65.8	-180	-179	82.44	90.34
Europa Campaign 1	COT 1	07E01	O	08-May-2026 22:00:08	1442	3.79	10:27:25	65	169	62	66.3	10.5	1.75	14.3	4.01	1.01	28.4	0.14	8.43	26.28	14.2	501.4	345	-176	-154	21.37	19.91
		08E02	O	23-May-2026 03:19:03	100	3.86	11:09:23	52	179	50	52.5	9.57	4.01	14.3	4	1	45.4	0.18	2.42	28.7	14.2	515.6	346	-157	-124	23.1	23.5
		09E03	O	06-Jun-2026 08:14:18	100	3.86	11:02:45	20	179	39	23.8	4.15	4.96	14.2	4	1	44.1	0.23	0.73	29.43	14.2	529.8	345	-125	-92.2	23.85	24.12
		10E04	I	20-Jun-2026 13:10:33	50	3.86	10:56:08	-14	178	29	21	-2.8	4.27	14.2	4	1	44.1	0.27	0.74	30.17	14.2	544	344	-93.6	-60.2	24.11	24.01
		11E05	I	04-Jul-2026 18:06:12	35	3.86	10:49:21	-47	178	18	50	-8.9	2.07	14.2	4	1	43.8	0.32	0.28	30.45	14.2	558.2	343	-61.3	-26.8	23.69	23.34
	Non-res	12E06	I	18-Jul-2026 22:46:06	25	3.88	12:10:11	-47	200	7.8	47	-15	0.32	12.5	7.11	2.11	44.7	0.36	0	30.46	25.2	572.4	341	-25.3	-0.56	24.48	31.69
	COT 2	14E07	O	13-Aug-2026 04:27:59	1231	3.96	11:14:06	-32	150	11	34.1	19.3	0.95	14.2	4	1	108	0.47	0.79	31.25	14.2	597.7	18.4	-180	171	33.91	27.59
		15E08	O	27-Aug-2026 09:06:54	25	3.95	13:12:44	-67	182	21	68.3	14.7	3.68	14.2	4	1	45.1	0.51	3.3	34.54	14.2	611.9	16.1	170.3	139.9	25.6	26.13
		16E09	O	10-Sep-2026 14:03:37	50	3.97	13:01:44	-37	180	32	40.1	10.3	5.46	14.2	4	1	43.6	0.56	4.08	38.62	14.2	626.1	15.1	140.6	111.7	26.46	26.81
		17E10	O	24-Sep-2026 19:01:07	50	3.98	12:54:49	-9	179	43	16.2	3.52	5.9	14.2	4	1	42.8	0.6	3.91	42.53	14.2	640.3	14.1	112.9	84.46	26.98	27.03
		18E11	I	08-Oct-2026 23:59:09	100	3.98	12:47:47	19	178	55	22.7	-3.7	4.96	14.2	4	1	41.8	0.64	4.94	47.47	14.2	654.5	13.1	85.93	58.02	26.92	26.6
		19E12	I	23-Oct-2026 04:55:41	25	3.97	12:40:44	47	177	67	48.5	-9.8	2.79	14.2	4	1	42.4	0.68	1.66	49.13	14.2	668.7	12	59.47	29.4	26.21	25.72
	Non-res	20E13	I	06-Nov-2026 09:57:57	218.9	3.94	12:16:52	77	172	79	77.2	-13	0.62	14.3	4.07	1.07	43.7	0.73	8.68	57.81	14.5	682.9	11.2	31.04	1.67	24.53	23.76
	COT 3	21E14	O	20-Nov-2026 20:43:35	891.9	3.85	15:05:27	82	191	92	84.8	10.7	2.3	14.2	4	1	51.5	0.78	6.12	63.93	14.2	697.3	34.2	178.4	-154	19.07	19.88
		22E15	O	05-Dec-2026 01:57:58	100	3.9	14:22:32	51	180	106	59.7	9.34	4.56	14.2	4	1	44.2	0.82	0.2	64.13	14.2	711.6	34.2	-156	-122	22.41	22.87
		23E16	O	19-Dec-2026 07:00:05	100	3.91	14:16:14	20	179	120	38.9	3.72	5.53	14.2	4	1	42.2	0.87	0.17	64.3	14.2	725.8	33.4	-125	-92.6	23.57	23.76
		24E17	I	02-Jan-2027 12:01:25	100	3.91	14:11:51	-11	178	136	34.3	-3.3	4.99	14.2	4	1	41.6	0.91	10.25	74.55	14.2	740	32.6	-95.3	-63.2	23.86	23.86
		25E18	I	16-Jan-2027 16:37:40	35	3.94	13:57:24	-47	177	151	53.3	-11	2.96	14.2	4	1	42.5	0.95	3.75	78.3	14.2	754.2	30.1	-59.8	-28.6	25.37	24.96
	Petal Rotation	26E19	I	30-Jan-2027 21:36:39	50	3.93	13:33:39	-79	172	167	79.5	-14	0.2	14.3	4.08	1.08	43.8	0.99	6.3	84.6	14.5	768.4	29.1	-29.6	3.14	24.24	23.59
		27E20	O	14-Feb-2027 09:47:43	50	4.03	14:25:29	5.3	155	176	36.8	11.9	0.42	17.8	4.94	0.94	54.2	1.05	19.03	103.6	17.6	782.9	58.6	177.3	179.4	28.97	16.46
		28E21	I	03-Mar-2027 23:11:06	100	4.08	16:09:27	-0	203	156	62.4	-16	0.46	14.3	4.1	1.1	36.4	1.08	0.74	104.4	14.6	800.4	37.1	-0.19	-0.04	18.75	30.64
		29E22	O	18-Mar-2027 12:19:17	25	4.02	15:15:33	-0	156	140	48.9	12.1	0.45	17.7	4.95	0.95	56.7	1.14	3.72	108.1	17.6	815	71.1	-180	179.9	28.96	16.19
		30E23	I	05-Apr-2027 02:00:36	82.26	4.03	16:58:06	0.2	201	122	74.5	-14	0.46	14.3	4.1	1.1	37.1	1.18	0	108.1	14.5	832.6	50.8	0.09	-0.03	17.15	29.42
		31E24	O	19-Apr-2027 14:54:09	25	4.01	16:06:01	0.2	156	108	61.5	12.9	0.47	17.8	4.95	0.95	56.5	1.23	1.48	109.6	17.6	847.1	84.1	-180	-180	29.07	16.28
		32E25	I	07-May-2027 04:36:27	44.27	4.02	17:49:23	7	202	91	87.5	-13	0.84	14.3	4.07	1.07	37.3	1.27	12.62	122.2	14.5	864.7	63.9	-0.42	-3.37	16.98	29.54
Transition to Europa Campaign 2	Petal setup	33E26	O	21-May-2027 15:19:36	1932	3.77	04:46:08	-27	343	79	106	10	0.32	13.5	4.53	1.35	53.7	1.33	0	122.2	16.1	879.1	87.9	-173	175.5	13.24	19.37
		34C01	O	06-Jun-2027 18:09:15	135.3	4.84	18:57:14	17	72.2	65	104	129	2.24	18.9	0.92	0.52	64.8	1.39	0	122.2	15.4	895.2	213	179.9	-176	115.2	103.4
		06G05	I	22-Jun-2027 03:54:43	1302	4.71	19:30:12	32	252	53	109	-64	0.19	12.9	3.3	1.82	1.51	1.39	0	122.2	23.6	910.6	38.2	5.76	-0.76	70.98	80.81
	Callisto Petal Rotation	37C02	I	15-Jul-2027 19:18:47	25	3.62	05:08:11	1.5	106	35	103	-120	0.27	20.3	1.56	1.56	44.6	1.44	0	122.2	25.9	934.3	332	0.6	-0.02	115.7	94.56
		38C03	O	10-Aug-2027 17:09:18	1614	3.61	04:32:20	0.1	260	15	112	114	0.27	14.9	2.3	2.3	5.06	1.44	0	122.2	38.4	960.2	170	180	180	94.59	108.4
		41C04	I	18-Sep-2027 03:33:46	1633	3.62	01:05:15	0	102	13	164	-114	0.27	20.4	1.56	1.56	22.9	1.46	0	122.2	25.9	998.6	275	0	0	108.3	94.62
		42C05	O	14-Oct-2027 01:32:12	543.2	3.63	00:37:28	0	258	34	171	118	0.27	13.7	1.26	1.26	5.13	1.47	0	122.2	21.1	1025	113	180	-180	94.57	112.5
		44C06	I	04-Nov-2027 04:06:49	1292	3.63	20:45:31	-1	106	51	131	-121	0.42	18.7	2.59	2.59	17.8	1.49	0	122.2	43.2	1046	206	0	0.34	112.7	97.97
		46C07	O	17-Dec-2027 09:03:01	2772	3.63	20:45:12	-29	257	89	125	115	2.37	15.2	1.59	1.54	10.6	1.5	0	122.2	26.6	1089	55.2	-180	174.9	97.77	107.3
	EC2 setup	35G06	I	12-Jan-2028 23:40:26	4657	3.2	20:13:34	-29	52.5	115	118	-36	0.74	19.4	3.13	1.39	11.4	1.51	0	122.2	22.4	1115	248	-10.3	-3.12	58.32	46.1
		49C08	O	04-Feb-2028 08:29:36	5644	4.37	18:58:30	0.3	258	138	105	116	0.78	16.7	1	1	12.6	1.52	0	122.2	16.7	1138	27.6	178.3	178.3	100.4	105.5
		50C09	O	21-Feb-2028 00:23:48	176.2	4.38	18:12:10	1.3	248	157	93.1	134	0.71	12	1.25	1.54	13.5	1.54	0	122.2	20.9	1154	25.8	178.3	178.5	105.5	120
Europa Campaign 2	LE	52E27	I	12-Mar-2028 21:45:26	382.8	4.03	16:50:28	-28	32.4	178	73.8	-19	0.49	14.3	4.1	1.1	68.2	1.6	0	122.2	14.6	1175	219	-8.03	0.39	37.27	27.71
		53E28	O	27-Mar-2028 11:09:09	148.1	4.16	03:08:12	-19	152	163	129	17.5	1.32	17.8	5	1	57.3	1.66	12.61	134.8	17.8	1190	254	179.4	169.5	32.9	22.65
		54E29	O	14-Apr-2028 05:18:42	25.68	4.16	15:06:55	16	333	144	49.7	17.2	0.51	14.1	3.89	0.89	42.9	1.7	0	134.8	13.8	1208	253	170.1	179.7	20.98	32.18
		55E30	I	28-Apr-2028 00:28:50	25.57	4.26	16:01:47	5.6	29	130	60.9	-17	0.24	17.8	5.02	1.02	33.7	1.74	29.44	164.2	17.8	1221	211	0.4	-2.14	35.77	24.36
	COT 4	56E31	I	15-May-2028 20:04:52	27.38	4.05	14:22:36	-61	359	112	64.8	-4.9	2.99	17.8	5.01	1.01	44.8	1.78	5.75	170	17.8	1239	216	0.4	56.15	13.63	13.48
		57E32	O	02-Jun-2028 15:16:52	126.1	4.04	14:33:48	35	359	96	51.9	4.31	1.42	17.8	5.01	1.01	42.9	1.83	0	170	17.8	1257	219	92.37	157.6	11.19	11.13
	COT 5	58E33	O	20-Jun-2028 10:27:47	246.5	4.13	04:47:57	88	210	80	92.8	11.6	1.19	17.8	5	1	43.1	1.87	4.2	174.2	17.8	1275	222	166.9	-159	18.53	19.03
		59E34	O	08-Jul-2028 04:52:24	27.12	4.17	02:48:22	56	180	65	117	10.5	3.49	17.8	5	1	42.3	1.91	0	174.2	17.7	1293	221	-161	-128	20.9	21.22
		60E35	O	25-Jul-2028 22:42:24	25.31	4.14	02:35:35	19	179	51	139	3.94	4.24	17.8	5	1	40.8	1.95	0	174.2	17.8	1310	219	-125	-89.3	19.87	20.18
		61E36	I	12-Aug-2028 16:59:55	25.19	4.15	02:29:56	-14	179	37	139	-2.4	3.54	17.8	5	1	40.5	1.99	0.33	174.5	17.8	1328	218	-93.7	-58.2	20.15	20.13
		62E37	I	30-Aug-2028 11:18:38	26.72	4.14	02:23:45	-48	178	24	121	-7.7	1.42	17.8	5	1	40.8	2.03	0.56	175.1	17.8	1346	217	-62.1	-24.6	19.33	18.97
		63E38	I	17-Sep-2028 05:24:09	26.98	4.13	03:29:46	-52	196	10	110	-13	0.83	16	9.06	2.06	41.2	2.07	3.13	178.2	32.2	1364	215	-24.5	4.16	19.03	25
	Petal	65E39	O	19-Oct-2028 10:08:02	575.4	4.01	14:19:38	16	337	15	39.2	11.7	0.39	14.1	3.91	0.91	93.4	2.17	0	178.2	13.9	1396	236	173.6	-178	16.89	26.21
	COT 6	66E40	I	02-Nov-2028 07:25:42	77.8	4.03	13:54:01	72	3.53	26	76.7	-16	2.45	14.2	4	1	35	2.2	3.15	181.4	14.2	1410	203	-1.42	-28.4	27.75	26.97
		67E41	I	16-Nov-2028 12:23:57	76.57	4.02	13:33:02	45	359	37	52.2	-12	4.49	14.2	4	1	44.6	2.25	2.89	184.2	14.2	1424	202	-29.1	-57.4	26.47	26.12
		68E42	I	30-Nov-2028 17:22:29	75.25	4.01	13:26:26	16	358	49	28.6	-5.5	5.3	14.2	4	1	43.2	2.29	2.33	186.6	14.2	1438	201	-58.7	-87.6	25.82	25.7
		69E43	O	14-Dec-2028 22:20:36	75.15	4	13:20:17	-13	358	61	22.3	2.26	4.67	14.2	4	1	42.5	2.33	2.91	189.5	14.2	1452	200	-89	-118	25.74	25.93
		70E44	O	29-Dec-2028 03:17:56	76.37	4.01	13:13:58	-42	357	73	42.3	9.13	2.77	14.2	4	1	43.3	2.38	0.04	189.5	14.2	1467	199	-119	-147	26.2	26.57
		71E45	O	12-Jan-2029 08:09:09	27.56	4	12:43:34	-65	351	86	62.9	13.7	0.1	14	4.19	1.21	44.5	2.42	0	189.5	14.9	1481	198	-147	-175	26.61	28.1
Disposal	Disposal	48G07	O	27-Jan-2029 05:24:04	1142	6.64	00:19:51	7	90.2	100	174	84.2	0.46	20.2	2.57	0.57	61.5	2.48	0	189.5	18.4	1496	272	-180	-179	90.58	84.21
		72G08	I	14-Feb-2029 13:43:49	600	6.6	07:02:24	87	349	119	91.9	-78	3.92	19.9	5	1	1.96	2.48	0	189.5	-	1514	114	0.67	-6.89	83.91	83.98

Table 1: Tour 18F17-beta events.

south. Places flybys over Thera and Thrace Macula (chaotic terrains displaying dark irregular features located near 180 W and 50 S [14]). The first flybys could be used for calibration (see Section III.i). The final transfer is a 9:2 resonance to avoid key activities (i.e., maneuver and/or flybys) during the solar conjunction, when communication with the spacecraft will not be reliable.

NR Non-resonant transfer to move the flyby location from the incoming leg to the outgoing leg of the spacecraft orbit.

COT-2: Uses 4:1 COT to cover the anti-Jovian hemisphere from south to north.

NR Non-resonant transfer to move the flyby location from the incoming leg to the outgoing leg of the spacecraft orbit.

COT-3: Uses 4:1 COT to cover the anti-Jovian hemisphere from north to south.

Petal Rotation: Uses $4 : 1^{+}/5 : 1^{-}$ petals to rotate the location of closest approach counterclockwise (as seen from Jupiter's north pole) along Europa's orbit (increasing L_{Eu}). Obtains sets of near-equatorial ground-tracks over panels 1 and 3.

Transition to Europa Campaign 2: Uses low-TID (Total Ionizing Dose) Callisto petal rotation with Ganymede leveraging to flip the location of closest approach to the opposite side of Europa's orbit (changing L_{Eu} by $\sim 180^{o}$).

Leading Edge: Uses 4 Europa flybys (3 on the sunlit sub-Jovian hemisphere) to set up COT4. E29 is the outgoing pump-down $(5 : 1/4 : 1)$ flyby for leading edge (LE) coverage.

COT-4: Uses 5:1 COT to cover the sub-Jovian hemisphere from south to north.

COT-5: Uses 5:1 COT to cover the dark side anti-Jovian hemisphere from north to south to obtain coverage of the same terrain, both lit and unlit, for E-THEMIS. Ends with a 9:2+ transfer to avoid solar conjunction and pump-down.

Pump-Down 2 Uses 1 Europa flyby and one petal rotation to pump-down into a 4:1 orbit and rotate the location of closest approach closer to Jupiter conjunction.

COT-6: Uses 4:1 resonant transfer to Europa to cover the sub-Jovian hemisphere from north to south.

Disposal: Uses Ganymede resonant hopping to increase the apojove such that, on the last orbit, solar gravity perturbations reduce the perijove for a planned Jupiter impact.

III.i Tour characteristics

This section discusses the main characteristics of 18F17-beta, and how it meets Enhancements 1-3, using the techniques explained in section IV. Tour 18F17-beta is build on the legacy of previous tours, especially 17F12 and 17F13, as shown in Fig. 5. All three tours are designed from a Earth-Jupiter direct interplanetary trajectory launching in 2022, and have almost identical pump-down, COT-1 and COT-2 sequences. Tour 17F13 branches off 17F12 with a third anti-Jovian COT-3, which was added to respond to anomalies such as missed observations due to off nominal operations, or to react to key observations from a previous flyby, at the cost of an ˜250 kRad.[2]

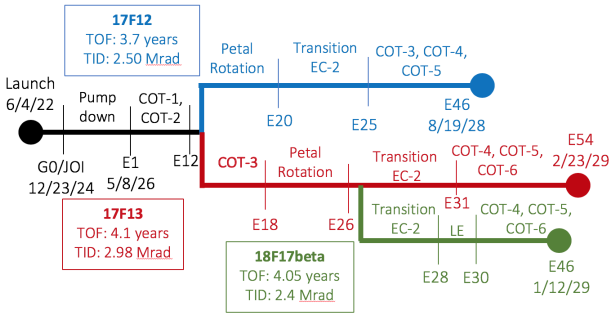

Fig. 5: Schematic of tour options.

The Europa Campaign 1 of 18F17-beta is the same as 17F13, however, we adopt a new strategy to meet Enhancement 2, where the early flybys of COT-1 are used for calibration and flight system testing, and the science potentially lost is then recovered during part of the COT-3 flybys. The same strategy could be applied to 17F13.

To make up for the 250 kRad of COT-3, 18F17-beta implements a new type of transition to EC-2 phase, where one Callisto flyby quickly pumps up the perijove outside the high-radiation region. Then a Ganymede flyby leverages down the v_{∞} at Callisto, and sets up a time-optimal Callisto petal rotation. At the end of the petal rotation, the process is reversed and the spacecraft returns to Europa at the desired location (about 180^{o} away), with the desired v_{∞} and

period . The TID cost of this phase is just 0.2 Mrad (including the setup flybys) compared to the 0.5 Mrad of typical switch-flip transitions, for about the same ΔV and time of flight (TOF). The TID savings are sufficient to offset the COT-3 costs, and to set-up the leading edge (LE) flyby.

After the Transition to Europa Campaign 2 Phase, a couple of Europa flybys sets up the outgoing 5:1/4:1 pump-down flyby that meets the LE constraints of Enhancement 1. Then the tour proceeds to COT-4 (lit sub-Jovian hemisphere coverage) and COT-5 (dark anti-Jovian hemisphere coverage), a sequence of flyby that spans 360^o crank angle, using 5:1 resonant transfers to meet the lower cadence goal for part of the EC-2, and to further reduce the TID. The lower cadence COTs are added in the second part of the tour, because in the first part of the tour, higher period orbits with the perijove toward the Sun would produce long eclipses. The 5:1 COTs conveniently follow the LE flyby, both techniques requiring a similar $v_\infty \sim 4.1$ km/s. This v_∞ is slightly higher than the one used in COT-1-3 (3.9 km/s), although not high enough to guarantee the same number of ground-tracks with a different resonance. Coarser ground-tracks are acceptable for the dark COT (preferable in terms of TID), but to make up for the few lit-flyby in COT-4, a denser ground-track sequence is implemented in COT6 with 4:1 resonances at the same v_∞.

Tour	17F12_V2	17F13	18F17-Beta
Launch Date	6/4/2022	6/4/2022	6/4/2022
Arrival Date	12/23/2024	12/23/2024	12/23/2024
Tour Duration (years)*	3.7	4.1	4.05
Number of Flybys			
Europa	46	54	45
Ganymede	4	4	6+
Callisto	9	9	9
No. of Night Side Europa Flybys	9	10	7
No. of Jupiter Orbits*	70	84	71
Time between Flybys (days)			
Maximum	229.0	229.0	229.0
Minimum	5.4	4.2	13
Minimum (Europa-to-Europa)	10.1	10.6	13.9
Deterministic ΔV, post-PRM (m/s)	182	188	189
Total Deterministic ΔV (m/s)	1,305	1,310	1,339
Maximum Inclination (deg.)	18.9	18.0	5.9
No. of Jupiter Eclipses	47	55	62
Maximum Eclipse Duration (hours)	9.15	9.14	9.20
Total Ionizing Dose (Mrad)	2.50	2.98	2.39

(*) From **G0** to EOM (last Europa flyby)

Table 2: Tour comparisons

Overall, 18F17-beta requires similar ΔV, TID, and TOF of the current baseline 17F12 (see Table 2), and also include the enhancement described in the introduction, at varying degrees. The improvements came by implementing new design strategies, built on techniques that will be explained in the following sections. 18F17-beta has passed the preliminary navigation analysis, and is currently being analyzed for its science return, after which it may be tweaked or re-designed in part. 18F17 has a similar number of Europa flybys as 17F12, with the additional COT-3 and the LE flybys, but without the Europa flybys in the Transition to EC-2 Phase.

IV. Tour techniques

IV.i Radiation environment for tour design

Spacecraft in orbit around Jupiter must contend with Jupiter's harsh radiation environment. A commonly used metric of how severely a spacecraft is impacted by the radiation is the TID received by a hypothetical silicon target at the centre of a 100-mil thick spherical shell of aluminum, of inner radius 8 inches. Computing this TID accurately is a laborious process, making it difficult to quickly compare the TID on different trajectories, an ability which would guide the mission design much more effectively. Here we develop a tool called GRAV2p (GRID2p, Averaged) to approximate the TID almost instantaneously, using a TID rate database computed with two previously developed tools and one averaging process.

First, the gridded version, GRID2P,[12] of GIRE2p[13] (the Galileo Interim Radiation Environment, version 2p) is used to quickly compute the electron and proton fluences at any particular point around Jupiter in System III coordinates (essentially body-fixed radius, latitude and longitude, with rotational period being the radio-emissions rotation period). There is no time-varying component. The next step is to average out the fluences over the longitude, since Jupiter's rotational period is much higher than the angular rate of most spacecraft trajectories that might be considered for tour designs, and the longitudinal variation is relatively slight, arising primarily from Jupiter's roughly 10-degree dipole tilt. The final step is to determine the TID that results at a given radius and latitude from exposure to these longitude-averaged fluences. Here another simplification is made in that the radiation transport is estimated by means of a response function rather than a full run of a radiation transport code.[14] The response function is generated by running the transport code NOVICE[15] for a small number of samples within each energy bin; the average TID per particle from the samples is then multiplied by the fluence in the energy bin to give the TID rate for that energy

bin.

The overall TID rate is then just the sum of the TID rates in each of the energy bins. After these three steps, we are left quite simply with the approximate TID rate at any point in space around Jupiter (Fig. 6), which can be integrated almost instantaneously over a trajectory to give the overall TID for that trajectory (similarly to what done in[16,17]). In spite of the numerous approximations made, the TID thus obtained for Jovian satellite tours is typically within a few percents of the accurately computed value.

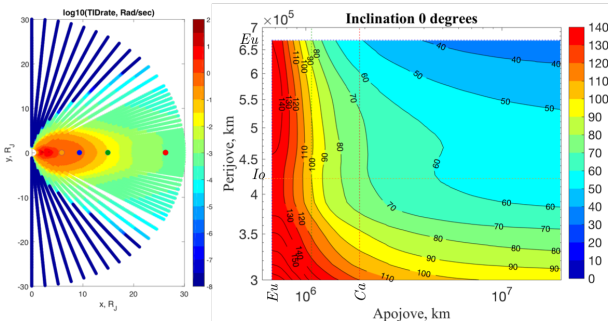

Fig. 6: On the left, longitude-averaged TID rate around Jupiter (100 mils Al spherical shell). Orbital radii of Io, Europa, Ganymede and Callisto are shown. On the right, TID per orbit

IV.ii (V-infinity, resonance) graph

In the circular moon orbit model, the spacecraft orbit can be described by two coordinates only, such as semi-major axis and eccentricity, or by v_∞ and resonance ratio, ρ. Features of the orbit (such as period, radiation dose, etc...) can be expressed directly as functions $F(\rho, v_\infty)$, and represented with level-sets on a (ρ, v_∞) two-dimensional graph. Figures 7, 8, and 10 show different examples of this graph, where (ρ, v_∞) are relative to Ganymede, Europa, Callisto, respectively. Because the graph can easily get cluttered with level-sets, the three figures highlight different features. In practice, one would hide or show only the features needed for a specific part of the tour design.

Figure 7 shows the basic features of the graph. The vertical lines with $\rho = n/m$ are the $n : m$ resonant orbits. The shadow region around the $2 : 1$ resonance is the $2 : 1$ attainable set, which is the collection of all the orbits that can be reached with a flyby (with a minimum-altitude constraint) from a $2 : 1$ orbit. An example minimum-altitude, pump-up flyby is shown with an arrow between point (b) and (c). Resonant orbits and their attainable sets are already included on a similar plot presented by Strange et al.[18]

Figure 7 also shows the range of v_∞ for a given resonant-hopping. For example, jumping between a 2:1 and a 4:1 at Ganymede is only possible for $3.5km/s < v_\infty < 4.5km/s$. At higher v_∞ the flyby bending is too small, and at lower v_∞ the $2 : 1$ and $4 : 1$ pump angles are too far apart (a consequence of the pump angles being close to 0^o). Note that the 2:1 attainable set reaches the 4:1 resonance at the same v_∞ at which the 4:1 attainable set reaches the 2:1 resonance (because pump-up and pump-down flybys are symmetric). We exploit this fact by only plotting the right or left boundary of the attainable sets, since information about the other bound can be deducted using neighboring resonances. For example, the know $v_{\infty max}$ to pump-up between 4:1 and 10:1 is about 6.5 km/s, because that's where the 4:1 pump-down attainable set reaches the 10:1 resonance. Figure 7 also shows $3 : 2^{\pm}$ non-resonant orbits branching off from the $3 : 1$ resonant orbit at point (a).

Figure 8 shows the (ρ, v_∞) graph at Europa with some additional features: the radiation dose (per spacecraft revolution), and the number of flybys needed to complete a COT sequence (a function of (ρ, v_∞), as explained in[9]). We re-arrange this data to also generate the parametric COT analysis of Fig. 9.

Figure 8 also shows an example of resonant hopping that is very sensitive to the type of non-resonance used: the 3:1+/4:1- is possible for v_∞ as low as 4.1 km/s (point b), but 4:1/3:1 requires 4.5 km/s (point a), and while 3:1-/4:1+ needs $v_\infty > 4.5$ km/s. Note that changes of as little as 200 m/s in the v_∞ are relevant as they cost ˜20 m/s in leveraging maneuvers, which is 10% of the entire deterministic ΔV budget for the tour. Finally point (c) in the graph shows that the 4:1/5:1 pumping used in Europa Clipper tours requires $v_\infty \approx 4$ km/s, at which 4:1 COTs are dense but 5:1 COT are coarse. We used this property in the Europa Campaign 2 of 18F17 to design the lower-density, 5:1 COT 4, followed by the higher-density, 4:1 COT-6.

Finally, Fig. 10 shows the (ρ, v_∞) graph at Callisto with a level-sets of constant v_∞ at Europa and Ganymede. The graph is used to set up the Transition to Europa Campaign 2 phase. Towards the beginning of this phase, we would like the spacecraft transfer to Callisto and quickly reach a 1:1 resonant orbit, to escape the high-radiation region. The transfer is represented by a point on the $v_{\infty,Eu} = 4$ km/s level-sets. The graph shows that the only points on that curve within the 1:1 attainable set region have

high v_∞ , for which the flyby ΔV are small. Alternative solutions at lower v_∞ include reaching a non-resonant $2:2^-$ attainable set (instead of a 1:1); or reaching $1:1$ from a low $v_{\infty,Ga}$, using a Callisto-Ganymede-Callisto transfer. Both solutions are implemented in 18F17.

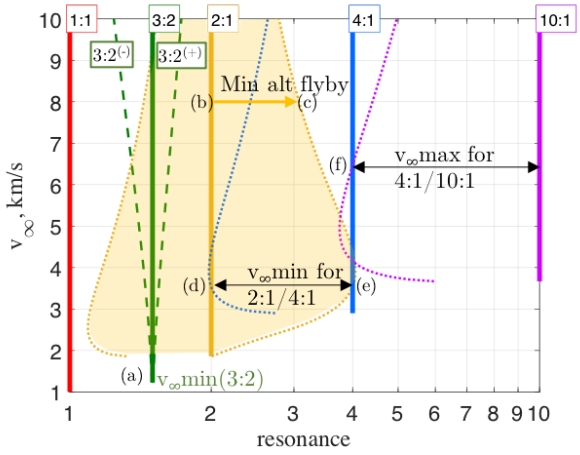

Fig. 7: (ρ, v_∞) graph at Ganymede. The flyby minimum altitude is 25 km.

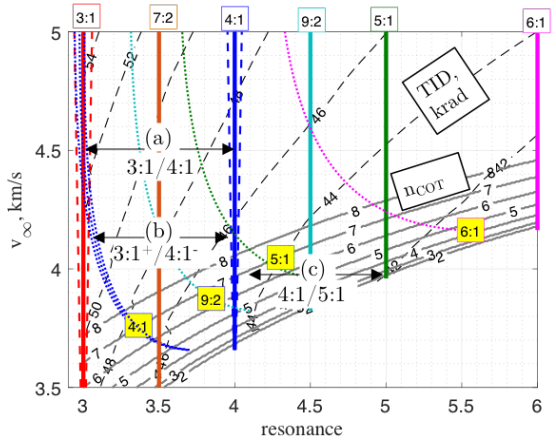

Fig. 8: (ρ, v_∞) graph at Europa. The flyby minimum altitude is 25 km.

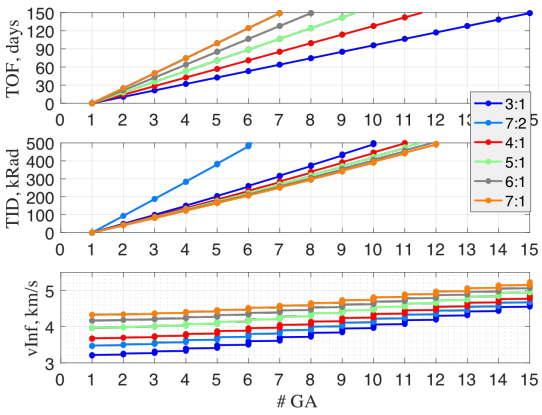

Fig. 9: Parametric COT analysis using functions of (v_∞, ρ)

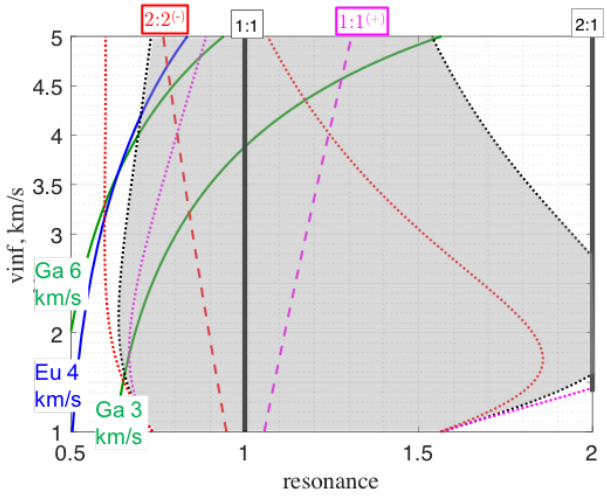

Fig. 10: (ρ, v_∞) graph at Ganymede. The flyby minimum altitude is 25 km.

IV.iii Fast and Low-TID rotations with cycler, switch-flip, or petals

Tours often need to rotate the spacecraft orbit relative to the Sun (for example for magnetic field and plasma measurements) or the location of the flybys on the satellite orbits (for example to measure high-order gravity fields coefficients and tidal effects; or for close-up surface observations at prescribed illumination conditions; or for distant measurements of the limbs at high phases at different longitudes). The Transition to EC-2 - present in all Europa Clipper tour designs, including 18F17 - is an example of a $\sim 180^o$ rotation, which is nearly ballistic and is designed to minimize the TID and TOF. This section discusses three techniques we analyzed for its design.

The first technique is Ganymede-Callisto cyclers. Cyclers are trajectories repeatedly transferring a spacecraft between two bodies. Figure 11 shows an example cycler optimized in a high-fidelity model (jTOP), with two cycles each providing $\sim 90^o$ rotation. First guess solutions are designed with the help of Star.[19]

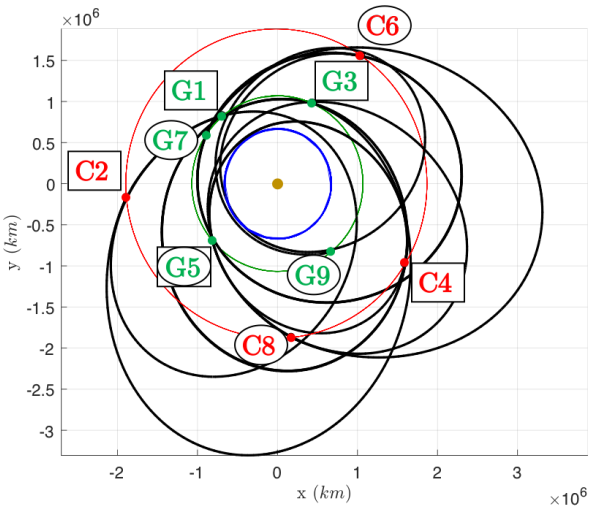

Fig. 11: 180^o rotation of the spacecraft orbit and of the flyby location, from G1 to G9, repeating two GCGC cycles (G1-G5 and G5-G9) .

The second technique uses a Callisto π-transfer sequence with 1:1 resonant transfers. The number of flybys in the sequence, and therefore its total TOF and TID, is function of the v_∞ and is computed with the same formula used in the COTs parametric analysis.

The third technique uses Callisto petal rotation[‡]. Figure 12 shows the TOF and TID for 180^o rotation for different families[§], most of them providing a clockwise rotation, with the exception of the $1:1^+/2:1^-$ family. Clockwise rotations exploit the apparent motion of the Sun (2.5^o per month), and can complete the 180^o rotation sooner. The figure also shows the switch-flip TOF and TID for comparison.

[‡]Options using Ganymede petal rotation were analyzed but not reported here as they were found to be less competitive than the Callisto petal.

[§]Selected looking at the attainable resonance sets on a $(\rho - v_\infty)$ graph

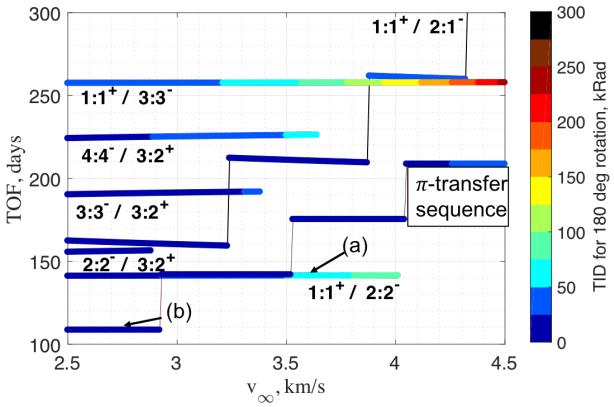

Fig. 12: 180^o rotation of the spacecraft orbit using Callisto petals or switch-flips. (a) is the design point for 18F17-Beta, (b) is the design point for 17F12 .

All these techniques can be used for the Transition to EC-2 Phase. The total TID and TOF costs will depend on their ease of implementation and their flexibility to satisfy operational constraints - which are not straight-forward to generically quantify. Instead this paper presents a qualitative discussion of the strengths and weaknesses of each approach, and some representative case studies, shown in Table 3. In 17F13, a π-transfer sequence is implemented as part of the Transition to EC-2; most of the TID is accrued during the Europa flybys before and after the switch-flip, from E26 to E33, which are needed to reach Callisto at low v_∞ and to crank the orbit down to zero inclination. The switch-flip TOF is penalized by 3:5 and 3:4 resonances, to pump up to 1:1, avoid flybys during the solar conjunction, and set up the proper phasing for the transfer to Europa. The petal rotation implementation is from the 18F17-beta tour, and uses Ganymede flybys before and after the petal to leverage the Callisto v_∞ to 3.6 km/s. The original strategy includes 3 pairs of 1:1+/2:2- petals; the first petal is changed into a 1:1+/3:3- to increase the time of flight between C03 and C04 when the solar conjunction occurs; and the last 1:1+ was replaced by a 2:2+ to obtain a more favorable phasing for G06 and eventually for the transfer to Europa.

Case	Feature	Cyclers	π Transfer Sequence	Petal Rotations
Rotation Only*	TID, krad	300	25	60
	TOF, mo	5.5	4	5
	v∞, km/s	3.5/4.5	2.7	3.6
Transition to EC2**	Phasing	Fixed v∞ and phasing	A few Eu-Ca options, adding 1:1 resonant transfers	Many Eu-Ca options by adjusting the ealry and final petals.
	Untarg. flybys	Can disrupt the phasing invalidating the trajectory	Mainly out-of-plan orbits with no untargeted flybys	Can be avoided changing the resonance (many options)
	Solar Conj.	Can disrupt the phasing invalidating the trajectory	Can be avoided changing the resonance (few options)	Can be avoided changing the resonance (many options)
	Eclipses	Few chance of mid eclipses	Few to no eclipses	Multiple eclipses for clockwise petals
	TID, krad	N/A	600	330
	TOF, mo	N/A	9.9	10.2

Table 3: Comparison of techniques and their implantation for 180^o rotation of the line of apses. (*) From the examples in the previous pictures. (**) Switch-flip from 17F13, Petal from 18F17-beta.

Finally, Fig. 13 shows the Callisto petal rotation of 18F17 (C02-C07) in the Jupiter-Callisto frame. The trajectory shadows three periodic orbits and their heteroclinic connections in the Callisto-Jupiter circular, restricted, three-body problems. Each periodic orbit is associated to a $n_1 : n_1/n_2 : n_2$ petal. These periodic orbits and their potential use for fast orbit rotations were discussed in Anderson.[10]

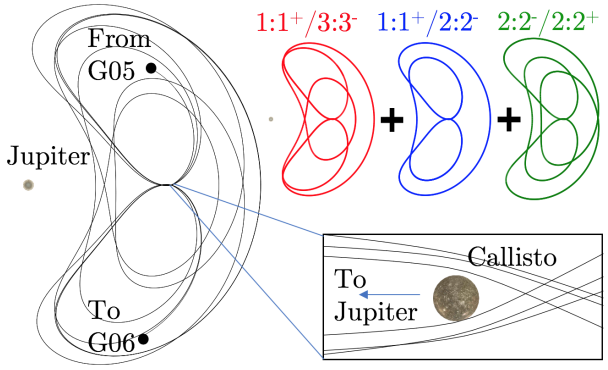

Fig. 13: Callisto petal rotation of 18F17 (C02-C08) in the Jupiter-Callisto rotating frame. The trajectory is symmetric and shadows a periodic orbit of the Jupiter-Callisto circular, restricted, three-body problems[10] .

IV.iv Leading and trailing point flyby

This section analyzes the conditions that enable close flybys over the leading and trailing regions. Figure 14 shows a flyby whose orbital plane contains the leading (and trailing) point. By identifying the position space and the velocity space, Fig. 14 also shows a great circle, which is the intersection of the flyby orbital plane on the v_∞ sphere, and contains both v_∞^- , v_∞^+, and the moon velocity vector. (v_∞^- , v_∞^+) are then connected by a pump-only flyby. In particular, a pump-up flyby flies over the trailing point, and a pump-down flyby flies over the leading point. The altitude of the passes h can be computed with

$$h = \frac{(e^2-1)\mu_{ga}/v_\infty^2}{1+e\sin\bar{\alpha}} - r_{ga} \qquad [1]$$

where $\bar{\alpha}$ is the average pump angle, and the eccentricity is given by

$$e = 1/\sin\frac{\delta}{2} = 1/\sin\frac{|\Delta\alpha|}{2}$$

$$\bar{\alpha} = \frac{\alpha^- + \alpha^+}{2}, \quad \Delta\alpha = \alpha^+ - \alpha^-$$

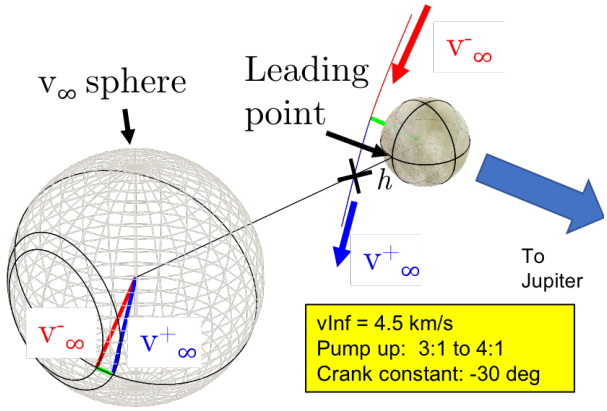

Fig. 14: Example of pump-up flybys

Since the altitude over the trailing and leading point does not depend on the crank angles, the following discussion assumes equatorial flybys with either $\kappa = 0$ (incoming flyby) or $k = \pi$ (outgoing flyby). The longitude of the closest approach is then

$$\lambda_{ELong} = -\bar{\alpha} * io + \pi\frac{1+io*du}{2}$$

$$io = \begin{cases} -1 & \text{for incoming } \kappa = 0 \\ +1 & \text{for outgoing } \kappa = \pi \end{cases}$$

$$du = \begin{cases} -1 & \text{for pump-down } \alpha^- < \alpha^+ \\ +1 & \text{for pump-up } \alpha^- > \alpha^+ \end{cases}$$

Finally, neglecting Europa eccentricity, the illumination conditions at the closest approach are a linear function of L_{Eu}

$$L_{Eu} = \frac{LST_{CA}}{24^h} 360^o - \lambda_{Elong} \qquad [2]$$

so that a constraint in LST is easily transformed into a constraint on L_{Eu}. Figure 15 shows a representation of these equations on Europa's surface. The leading-point region coverage is enabled by a low-altitude, pump-down flyby (incoming or outgoing), with $\bar{\alpha}$ as close as possible to 90^o. Figure 15 also shows the ground-track of the leading-edge flyby E29 in 18F17-beta. The spacecraft reaches 15^o from the leading point at < 2000 km (in fact, < 1000 km) with LST in the $9^h - 15^h$ bin, as required by Enhancement 1.

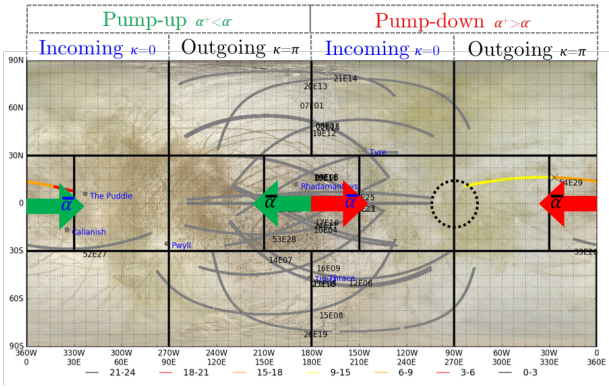

Fig. 15: Location of the closest approach for an equatorial flyby. Also plotted: ground-track of E29 flyby (below 1000 km) from 18F17-beta.

Leading-edge flyby implementation

A low-altitude leading-edge flyby is designed with a pair (α^-, α^+), such that $\bar{\alpha} \to 90^o$ ($\lambda_{Elong} \to 270^o$) and $\Delta\alpha \to \delta_{max}$ $(h \to h_{min})$. In practice, the flyby needs to be connect to other parts of the tour, and the pair (α^-, α^+) is chosen from a small set of resonant or non-resonant Europa transfers. Transfers shorter than 10 days are not considered due to operational constraints, and transfers with too many perijove passes are excluded for their large accrued TID. Low resonances such as 3:2 are also excluded for the TID needed to set them up. With these considerations and with the help of a (ρ, v_∞) graph, a short list of (α^-, α^+) is selected and for them, the altitude over the leading point is computed as function of v_∞. To meet the specific Enhancement 1 requirements, Eq. 1 and 2 are modified as

$$h_{15^o} = \frac{(e^2-1)\mu_{ga}/v_\infty^2}{1 + e\sin(\bar{\alpha} + \pi/12)} - r_{ga}$$

$$L_{Eu} = \frac{LST_{LE}}{24^h} 360^o - (270^o + io * 15^o)$$

where h_{15^o} is the minimum altitude at $15^o \equiv \pi/12$ off the trailing point. The illumination condition constraint becomes

$$LST \in [9^h, 15^h] \to$$
$$\to \begin{cases} L_{Eu} \in [-120^o, -30^o] & \text{for incoming } \kappa = 0 \\ L_{Eu} \in [-150^o, -60^o] & \text{for outgoing } \kappa = \pi \end{cases}$$

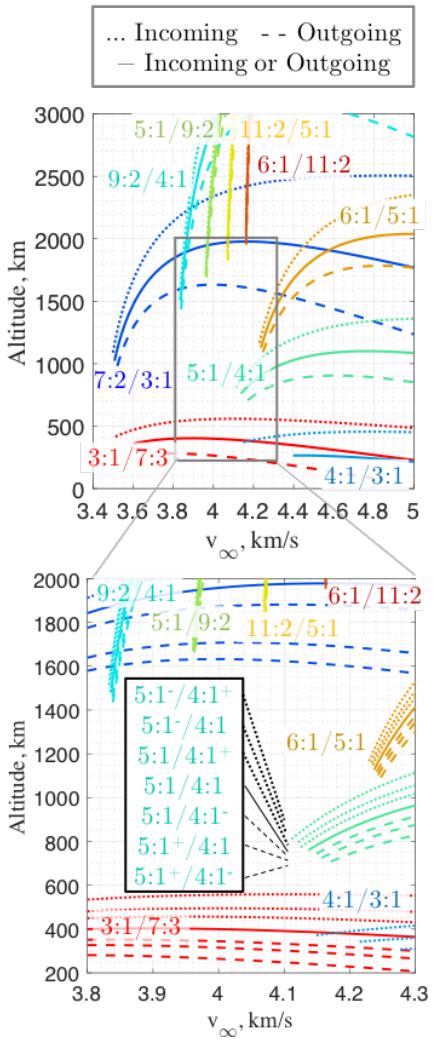

Fig. 16: Families of leading-edge flybys. The altitude if the lowest in a region up to 15^o away from leading point.

Note that the second constraint is the easier to meet, since outgoing L_{Eu} of -150^o are also acceptable for the sub-jovian COTs in EC-2. An outgoing

leading-edge flyby is a more efficient implementation (as opposed to a inbound flyby) when considering the high number of other science measurement requirements.

Figure 16 shows the altitude of the leading-point-region entry ($\lambda_{Elong} = 185^o$) as function of the v_∞, for several families of pump-down flybys. Each family is identified by the resonant or non-resonant transfers connected by the flyby. The figure on the left only shows the families $n_1 : m_1^-/n_2 : m_2^+$ (dotted line) , $n_1 : m_1/n_2 : m_2$ (solid line), and $n_1 : m_1^+/n_2 : m_2^-$ (dashed line). The figure on the right shows a close-up with all the possible combination of resonant and non-resonant transfers. 18F17-beta uses an outgoing $5 : 1/4 : 1^-$, since it can be easily patched to the rest of EC-2 , and doesn't require much TID.

V. Conclusion

This paper presents the candidate tour 18F17-beta for the Europa Clipper mission and the new techniques that are developed to meet (at various levels) the enhancements requested at the recent Preliminary Design Review. In particular, the tour includes a flyby covering the leading point region, and two lower-cadence COTs during the later part of the mission. The tour utilizes the same three COT sequences of 17F13, when only two are needed to meet the level-1 science requirements, as a way to (at worst) have a number of early flybys for calibration, and (at best) a way to offer robustness to the tour. The TID costs of the third COT sequence was compensated with a new, low-TID transition to Europa Campaign 2 phase, using Callisto petal rotations.

VI. Acknowledgments

This research was carried out at the Jet Propulsion Laboratory, California Institute of Technology, under a contract with the National Aeronautics and Space Administration. Copyright 2018 California Institute of Technology. Government sponsorship acknowledged.

References

[1] Hand, K. "Is there life on Europa?" Nature, , No. 457, pp. 384–385, 2009. doi: 10.1038/457384a.

[2] Lam, T., Buffington, B. B., and Campagnola, S. "A Robust Mission Tour for NASA's Planned Europa Clipper Mission." "2018 Space Flight Mechanics Meeting," American Institute of Aeronautics and Astronautics, Reston, Virginia, jan 2018. ISBN 978-1-62410-533-3. doi: 10.2514/6.2018-0202.

[3] Buffington, B. B. "Trajectory design for the Europa Clipper mission concept." "AIAA/AAS Astrodynamics Specialist Conference, AIAA paper 20144105," 2014.

[4] Buffington, B. B., Campagnola, S., and Petropoulos, A. E. "Europa multiple-flyby trajectory design." "AIAA/AAS Astrodynamics Specialist Conference 13 - 16 August 2012, Minneapolis, Minnesota AIAA 2012-5069," August. 2012. doi:10.2514/6.2012-5069.

[5] Lam, T., Arrieta-Camacho, J. J., and Buffington, B. B. "The Europa mission: multiple europa flyby trajectory design trades and challenges." "2015 AAS/AIAA Astrodynamics Specialist Conference, Vail, Colorado, August 9-13. Paper AAS-15-657," 2015.

[6] Scott, C., Ozimek, M., Buffington, B. B., and Roncoli, R. "ROBUST CAPTURE AND PUMP-DOWN DESIGN FOR NASA'S PLANNED EUROPA CLIPPER MISSION." "27th AAS/AIAA Space Flight Mechanics Meeting, At San Antonio, Texas, Paper No. AAS 17437," 2017.

[7] Campagnola, S. and Russell, R. P. "Endgame Problem Part 2: Multi-Body Technique and T-P Graph." Journal of Guidance, Control, and Dynamics, Vol. 33, No. 2, pp. 476–486, 2010. doi:10.2514/1.44290.

[8] Uphoff, C., Roberts, P. H., and Friedman, L. D. "Orbit Design Concepts for Jupiter Orbiter Missions." Journal of Spacecraft and Rockets, Vol. 13, pp. 348–355, 1976. doi:10.2514/3.57096.

[9] Buffington, B. B., Strange, N. J., and Campagnola, S. "Global moon coverage via hyperbolic flybys." 23rd International Symposium on Space Flight Dynamics, 2012.

[10] Anderson, R. L., Campagnola, S., and Buffington, B. B. "Analysis of Petal Rotation Trajectory Characteristics." Journal of Guidance, Control, and Dynamics, Vol. 41, No. 4, pp. 827–840, apr 2018. ISSN 0731-5090. doi: 10.2514/1.G002571.

[11] Campagnola, S., Ozaki, N., Sugimoto, Y., Yam, C. C. H., Chen, H., Kawabata, Y., Ogura, S.,

Sarli, B., Kawakatsu, Y., Funase, R., Nakasuka, S., Sugimoto, Y., Yam, C. C. H., Kawakatsu, Y., Chen, H., Kawabata, Y., Ogura, S., and Sarli, B. "Low-Thrust trajectory design and operations of procyon, the first deep-space micro-spacecraft." 24th International Symposium on Space Flight Dynamics, Munich, Germany, Vol. 7, 2015. ISSN 00741795.

[12] Evans, R. "A new GRID program, GRID2p, for quick estimates of Jupiter trapped particle fluences, Interoffice Memorandum 5132-15-032." Tech. rep., Jet Propulsion Laboratory, 2018.

[13] Garrett, H. B., Martinez-Serra, L. M., and Evans, R. "Updating the Jovian Proton Radiation Environment, Jet Propulsion Laboratory Publication 15-9." Tech. rep., 2015.

[14] Rasmussen, R., Evans, R., Jun, I., Kang, S., and Petropoulos, A. E. "Personal communication, Jet Propulsion Laboratory.", 2011.

[15] Jordan, T. "NOVICE: A radiation transport/shielding code, Experimental and Mathematical Consultants, Report EMP.L82.", 1982.

[16] Campagnola, S., Takashima, T., and Kawakatsu, Y. "Jovian radiation models for preliminary mission design." Tech. rep., JAXA/ISAS RAS-MDL-11002, 2011.

[17] Tardivel, S., Klesh, A. A. T., and Campagnola, S. "Average Daily Radiation Dose as a Function of Altitude, Latitude, and Shielding." Journal of Spacecraft and Rockets, Vol. 54, No. 6, pp. 1367–1375, nov 2017. ISSN 0022-4650. doi: 10.2514/1.A33790.

[18] Strange, N. J., Campagnola, S., and Russell, R. P. "Leveraging flybys of low mass moons to enable an Enceladus orbiter." "Advances in the Astronautical Sciences," Vol. 135, pp. 2207–2225. aug 2010. ISBN 9780877035572. ISSN 00653438.

[19] Landau, D. F. "Efficient Maneuver Placement for Automated Trajectory Design." "Astrodynamics Specialists Conference AAS 15-585," pp. 2427–2446. 2015.